Chymase inhibition prevents myocardial fibrosis through the attenuation of NOX4-associated oxidative stress in diabetic hamsters

Yasutaka Maeda[1], Toyoshi Inoguchi[1,2]*, Ryoko Takei[1], Hari Hendarto[1], Makoto Ide[1], Tomoaki Inoue[1], Kunihisa Kobayashi[1], Hidenori Urata[3], Akira Nishiyama[4], Ryoichi Takayanagi[1]

ABSTRACT

Aims/Introduction: Diabetic cardiomyopathy entails the cardiac injury induced by diabetes, independent of vascular disease or hypertension. Despite numerous experimental studies and clinical trials, the pathogenesis of diabetic cardiomyopathy remains elusive. Here, we report that chymase, an immediate angiotensin II (AngII)-forming enzyme in humans and hamsters, and NOX4-induced oxidative stress have pathogenic roles in myocardial fibrosis in diabetic hamsters.

Materials and Methods: Expression of chymase was evaluated in the hearts of streptozotocin (STZ)-induced diabetic hamsters. The impact of chymase-specific inhibitors, TEI-E00548 and TEI-F00806, on myocardial fibrosis, and increased levels of intracardiac AngII, accumulation of 8-hydroxy-2′-deoxyguanosine (an oxidative stress marker in urine and heart tissue) and expression of heart NOX4 in diabetic hamsters were investigated.

Results: Myocardial chymase expression was markedly upregulated in STZ hamsters in a glucose-dependent manner. A total of 8 weeks after STZ administration, the diabetic hamsters showed enhanced oxidative stress and NOX4 expression in the heart, in parallel with increased myocardial AngII production. Oral administration of chymase-specific inhibitors, TEI-F00806 and TEI-E00548, normalized heart AngII levels, and completely reversed NOX4-induced oxidative stress and myocardial fibrosis in STZ-induced diabetic hamsters, although they did not affect the activity of the systemic renin–angiotensin system or systolic blood pressure.

Conclusions: Chymase inhibition might prevent oxidative stress and diabetic cardiomyopathy at an early stage by reducing local AngII production. (J Diabetes Invest, doi: 10.1111/j.2040-1124.2012.00202.x, 2012)

KEY WORDS: Chymases, Diabetic Cardiomyopathies, Nicotinamide adenine dinucleotide phosphate oxidase

INTRODUCTION

Diabetic cardiomyopathy, characterized by diffuse myocardial fibrosis and myofibrillar hypertrophy without evidence of valvular, hypertensive or ischemic heart disease, is well established as a cause of heart failure in diabetic patients, independent of impaired systolic function. The risk of cardiovascular death or hospitalization for heart failure was significantly greater in diabetic patients with preserved systolic function than in those with systolic heart failure[1]. However, despite numerous experimental studies and clinical trials, the pathogenesis of diabetic cardiomyopathy remains elusive. Hyperglycemia and lipotoxicity associated with obesity or insulin resistance are thought to be the main causes of cardiac cell death and ventricular dysfunction in diabetes. Lipotoxicity, caused by elevated free fatty acid levels and compensatory triglyceride storage in cardiomyocytes, might explain the underlying mechanism. Therefore, we focused on oxidative stress, which modulates myocardial hypertrophy and apoptosis through upregulation of local angiotensin II (AngII) activity in the hyperglycemic state.

Many clinical trials have shown that blockade of the renin–angiotensin system (RAS) reduces cardiovascular mortality and morbidity[2,3], even in diabetic patients[4]. Localized RAS components, including myocardial AngII, were upregulated in association with cardiac cell death, myocardial fibrosis and hypertrophy in humans, and in animal models with diabetes[5,6]. Chymase, a serine protease, specifically hydrolyzes the Phe8–His9 bond in angiotensin I (AngI) to generate AngII in local tissues of several species, including humans and hamsters[7]. In the human heart, chymase has more potent AngII-forming activities than does angiotensin-converting enzyme (ACE), irrespective of the presence of myocardial infarction[8]. Similar to that in humans, hamster chymase is activated in the myocardium in response to hypertension, contributing to the development of ventricular fibrosis[9]. Several reports have shown that chymase is upregulated in the ischemic heart, and its inhibition improved

[1]Department of Medicine and Bioregulatory Science, Graduate School of Medical Sciences, [2]Innovation Center for Medical Redox Navigation, Kyushu University, Fukuoka, [3]Department of Internal Medicine, Fukuoka University, Chikushi Hospital, Chikushino, and [4]Department of Pharmacology, Faculty of Medicine, Kagawa University, Kagawa, Japan

*Corresponding author. Toyoshi Inoguchi Tel.: +81-92-642-5284 Fax: +81-92-642-5287
E-mail address: toyoshi@intmed3.med.kyushu-u.ac.jp

Received 26 October 2011; revised 10 January 2012; accepted 10 January 2012

survival and cardiac hypertrophy after myocardial infarction[8,10]. However, it is unclear whether chymase contributes to the development of diabetic cardiomyopathy.

In contrast, a recent *in vivo* study showed that aging and pressure overload induced oxidative stress in the heart, and caused cardiac dysfunction by upregulating NOX4, the major NAD(P)H oxidase isoform in cardiomyocytes[11,12]. Oxidative stress is an important pathogenic factor in the development of diabetic vascular complications, including cardiomyopathy[13–15]. Vascular NADPH oxidase, a major source of reactive oxygen species (ROS), is stimulated by high glucose or free fatty acid levels in a protein kinase C (PKC)-dependent manner[16–18]. Suppressing oxidative stress *in vivo* was reported to prevent diabetic cardiomyopathy[19,20]. Similarly, AngII mediates NADPH oxidase-dependent ROS production by activating PKC[21]. AngII-induced oxidative stress was also reported to be involved in the development of diabetic cardiomyopathy[14].

Considering these earlier findings, we hypothesized that chymase-dependent AngII production might play an important role in the worsening of oxidative stress in the diabetic heart, contributing to the development of diabetic cardiomyopathy. In the current study, we explored the pathological role of upregulated cardiac AngII and consequent NOX4-induced oxidative stress in cardiac myofibrosis in diabetic hamsters using chymase-specific inhibitors.

MATERIALS AND METHODS

Animals

Male Syrian hamsters (Japan SLC, Shizuoka, Japan) were given standard hamster chow and water *ad libitum*. Diabetes was induced in 8-week-old hamsters by intraperitoneally injecting streptozotocin (STZ; Sigma-Aldrich, St. Louis, MO, USA) in 0.1 mol/L citrate buffer, pH 4.5, at a dose of 30 mg/kg bodyweight, every 3 days for 2 weeks. Hamsters with fasting blood glucose levels >250 mg/dL were considered diabetic. Half of the diabetic hamsters were intraperitoneally implanted with osmotic minipumps releasing insulin U-500 (3 U/day; Eli Lilly and Company, Indianapolis, IN, USA) to achieve normoglycemia. The other half underwent sham operation. Hamsters were killed after 4 weeks of treatment by anesthesia, and their hearts were immediately excised and stored at −80°C. In a separate experiment, STZ-induced diabetic hamsters were orally administered with a chymase-specific inhibitor (TEI-E00548 or TEI-F00806; 10 mg/kg per day, provided by Teijin Pharma Ltd, Tokyo, Japan) mixed in normal hamster chow for 8 weeks. Heart rate and systolic blood pressure were measured at the left lower limb by a non-invasive modified tail-cuff method (BP Monitor for Rats and Mice, Model MK-2000; Muromachi Kikai, Tokyo, Japan). Urine samples were collected at week 8 and analyzed by enzyme-linked immunoassays (ELISA) to measure 8-hydroxy-2′-deoxyguanosine (8-OHdG; 8OHdG Check; Japan Institute for the Control of Aging, Fukuroi, Japan) and 8-iso-plastaglandin F2α (8-iso-PGF2α; Urinary Isoprostane ELISA Kit; MED.DIA s.r.l, San Germano, Italy). Values were adjusted for 24-h urine volume and bodyweight. To evaluate cardiac RAS component activity, hamsters were killed by decapitation, and their hearts were immediately dissected and frozen. Serum samples were obtained for biochemical assays. This study was approved by the Animal Care and Use Committee, Kyushu University.

Immunohistochemistry

Heart tissues were fixed in 10% formaldehyde and embedded in paraffin. Antigen retrieval was carried out in 10 mmol/L citrate buffer with 0.1% Nonidet P-40 (Sigma-Aldrich) in a microwave oven. Triton X-100 (0.1%) was used for cell permeabilization. Endogenous peroxidase was inactivated with 3% H_2O_2 in methanol. After blocking with 1% bovine serum albumin, sections were immunostained with rabbit polyclonal antihamster chymase antibody (8 μg/mL; Teijin Pharma Ltd.), anti-8-OHdG mouse monoclonal antibody (4 mg/mL; Japan Institute for the Control of Aging) and anti-human NOX4 goat polyclonal antibody (4 μg/mL; Santa Cruz Biotechnology, Santa Cruz, CA, USA). The density of 8-OHdG staining was analyzed using Adobe Photoshop (version 6.0; Adobe Systems, Mountain View, CA, USA), as previously reported[22].

Ribonucleic Acid Preparation and Quantification of Messenger Ribonucleic Acid Expression Levels

Total ribonucleic acid (RNA) was extracted from the frozen tissue samples, and messenger ribonucleic acid (mRNA) expression levels were quantified as we reported previously[23].

Western Blot Analysis

Western blotting of NOX4 was carried out as we described previously[23].

Assessment of Oxidative Stress in Heart Tissue

We quantified the peroxidation level in heart tissue homogenate using a commercially available kit for thiobarbituric acid reactive substances (TBARS) assay (Cayman Chemical Company, Ann Arbor, MI, USA). Results are expressed by pmol malondialdehyde (MDA) per mg total protein.

Morphology and Quantification of Collagen Protein in Myocardial Sections

Azan staining (Azan stain kit; Muto Pure Chemicals CO. Ltd, Tokyo, Japan) was carried out for the morphological analysis of myocardial fibrosis. We used a collagen staining kit (Cosmo Bio CO. Ltd, Tokyo, Japan) to quantify collagen protein accumulation in horizontal sections of the left ventricular (LV). After LV sections were stained with staining solution, we extracted the staining dye from the tissue sections using 200 μL of extract solution containing methanol and measured the absorbance at 530 nm (red) for collagen protein and 605 nm (green) for non-collagen protein, as described previously[24]. The mean percentage of collagen protein to non-collagen protein in 10 LV sections of each hamster was compared statistically. A 4-hydroxyproline

assay was used to measure the collagen content in the heart tissue homogenate using a commercially available kit (BioVision, Mountain View, CA, USA). Results are expressed by ng hydroxyproline per mg total protein.

Measurement of Serum RAS Components and Heart AngII Levels

We measured the serum RAS components using commercially available kits for AngII, renin activity, AngI and ACE, as we previously described[23]. Heart AngII was measured as previously described[25] using a method consisting of solid-phase extraction and radioimmunoassay (RIA).

Statistical Analysis

Data are means ± SEM. Statistical analysis was carried out with Student's *t*-test or one-way ANOVA with Fisher's protected least significant difference test. Values of $P < 0.05$ were considered statistically significant.

RESULTS

Chymase Expression Levels in the Diabetic Heart

We first determined the expression of chymase in heart tissues from STZ-induced diabetic hamsters (experiment 1). To elucidate the effect of diabetic state on chymase expression, we treated STZ-induced diabetic hamsters without or with intraperitoneal insulin infusion through osmotic minipumps. The characteristics of the hamsters are shown in Table 1. After 4 weeks of insulin infusion, the blood glucose levels were reduced to near-normal levels, whereas the untreated diabetic group showed severe hyperglycemia and marked weight loss. Immunostaining analysis showed that, in untreated diabetic hamsters, chymase expression was strongly enhanced in cardiomyocytes with the infiltration of chymase-positive cells into the pericardial serosa. Insulin infusion normalized the diabetes-induced overexpression of chymase (Figure 1a–d). Real-time

Table 1 | General characteristics of the control, streptozotocin-treated and streptozotocin + continuous intraperitoneal insulin infusion-treated hamsters

n	Control	STZ	STZ + CIPII
	8	8	8
10-weeks-old (before treatment)			
Bodyweight (g)	122.3 ± 1.6	123.3 ± 4.0	114.8 ± 3.1
Blood glucose (mg/dL)	95.0 ± 5.3	218.0 ± 28.8*	274.2 ± 24.1*
14-weeks-old (after treatment)			
Bodyweight (g)	162.3 ± 3.2***	129.0 ± 5.9**	158.8 ± 3.3***
Blood glucose (mg/dL)	94.7 ± 8.8	352.8 ± 30.4**,***	81.9 ± 6.7***

STZ, streptozotocin (STZ)-induced diabetic hamsters with sham operation; STZ + CIPII, STZ-induced diabetic hamsters with continuous intraperitoneal insulin infusion (CIPII). Data are means ± standard error of the mean. *$P < 0.01$ vs control (ANOVA); **$P < 0.01$ vs control and STZ + CIPII (ANOVA); ***$P < 0.01$ vs before treatment (paired *t*-test).

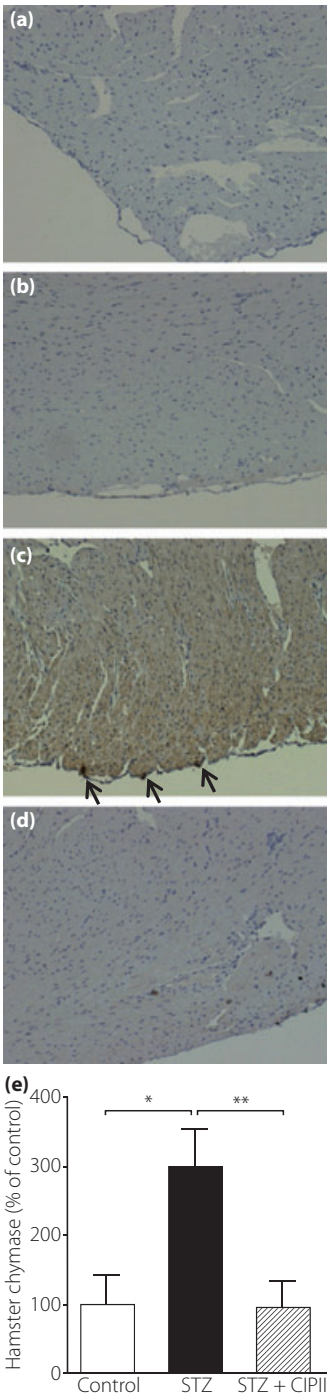

Figure 1 | Heart chymase expression in diabetic hamsters. (a–d) Immunohistochemistry for chymase expression in the heart. Brown, 3,3′-diaminobenzidine tetrahydrochloride staining (chymase); blue, hematoxylin counter-staining. (a) Negative control (b) control, (c) streptozotocin (STZ), streptozotocin-induced diabetic hamsters, (d) STZ + continuous intraperitoneal insulin infusion (CIPII); streptozotocin-induced diabetic hamsters treated with continuous intraperitoneal insulin infusion (magnification: ×200). (e) Quantification of hamster chymase messenger ribonucleic acid levels in the heart. Results are shown as a percentage of the controls. β-actin: internal control. White bars, controls; black bars, STZ; hatched bars, STZ + CIPII.

polymerase chain reaction (PCR) analysis showed that the mRNA levels of chymase were increased by 3.0-fold in the heart tissues from diabetic hamsters compared with the control hamsters. These increases were completely normalized by insulin infusion (Figure 1e).

Effects of Chymase Inhibition on RAS Component Activity

Next, we investigated the role of chymase in oxidative stress and cardiomyopathy in the heart of diabetic hamsters using two different orally active chymase-specific inhibitors (experiment 2). The biochemical properties of TEI-E00548 are reported in detail elsewhere[10]. Briefly, TEI-E00548 inhibits hamster chymase *in vitro* (Ki = 30.6 nmol/L) and has little effect on other serine proteases, including cathepsin G, elastase, chymotrypsin and trypsin (concentration at 50% inhibition was >1 mol/L). It did not inhibit ACE-dependent AngII formation. We also used another specific inhibitor, TEI-F00806, whose inhibition constant (Ki = 9.85 nmol/L) is approximately threefold greater than that of TEI-E00548. Both inhibitors (10 mg/kg per day) were orally administered to the diabetic hamsters for 8 weeks. The characteristics of the hamsters are shown in Table 2. There were no significant differences in general characteristics, including hemodynamic parameters, blood pressure and heart rate, between STZ-induced diabetic hamsters treated with or without chymase inhibitors. The major systemic RAS components were upregulated in STZ-induced diabetic hamsters, but were not affected by chymase inhibition (Figure 2a–c). Serum renin activity was significantly higher in STZ-induced diabetic hamsters ($P < 0.05$) than in the control hamsters, but not in either the TEI-E00548- or TEI-F00806-treated hamsters (Figure 2a). Serum AngI concentrations were significantly higher in the STZ-induced diabetic hamsters and the TEI-F00806-treated hamsters ($P < 0.01$) than in the control hamsters, but not in the TEI-E00548-treated hamsters (Figure 2b). Serum ACE activity was significantly higher in the STZ, TEI-E00548 and TEI-F00806 groups than in the control group (Figure 2c). Importantly, although chymase inhibitors had no effect on systemic AngII, they completely suppressed the overproduction of tissue AngII in the diabetic heart (Figure 2d,e). There were no significant differences in serum AngII concentrations between the control and STZ-induced diabetic hamsters (Figure 2d). In contrast, heart AngII levels were significantly higher in the STZ-induced diabetic hamsters vs the control hamsters ($P < 0.01$), but were lowered to the control levels by both chymase inhibitors (both, $P < 0.01$ vs STZ; Figure 2e).

Table 2 | Effects of chymase inhibition on general characteristics of streptozotocin-induced diabetic hamsters

n	Control	STZ	STZ+TEI-E00548	STZ+TEI-F00806
	8	8	8	8
10-weeks-old (before treatment)				
Bodyweight (g)	136.2 ± 5.2	116.6 ± 4.7**	119.3 ± 4.5**	126.8 ± 4.5
Blood glucose (mg/dL)	95.6 ± 6.8	287.2 ± 18.6**	276.8 ± 10.5**	286.2 ± 32.1**
Systolic blood pressure (mmHg)	90.3 ± 9.7	82.0 ± 5.5	104.7 ± 13.4	100.1 ± 6.2
Heart rate (per min)	369.9 ± 15.2	370.0 ± 19.3	382.9 ± 31.6	411.9 ± 33.0
18-weeks-old (after treatment)				
Bodyweight (g)	178.5 ± 2.3*	165.3 ± 1.3*	146.0 ± 9.0***	152.0 ± 16.0***
Blood glucose (mg/dL)	109.8 ± 7.2	315.1 ± 19.8**	279.2 ± 18.2**	316.0 ± 21.9**
Systolic blood pressure (mmHg)	118.9 ± 18.3	107.1 ± 7.9	104.3 ± 4.6	104.1 ± 3.6
Heart rate (per min)	427.1 ± 35.4	369.9 ± 31.9	391.0 ± 30.1	348.1 ± 38.2

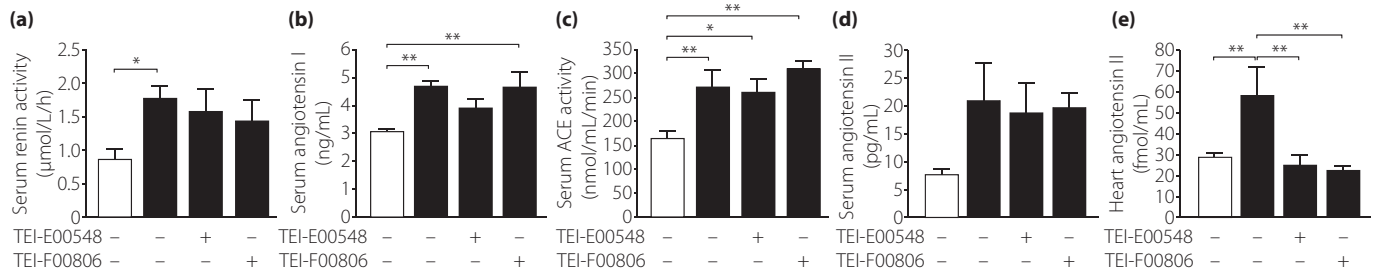

Figure 2 | Effects of chymase inhibition on the renin–angiotensin system. White bars: control, non-diabetic controls. Black bars: streptozotocin (STZ), STZ-induced diabetic hamsters. (a) Serum renin activity, (b) angiotensin I concentration, and (c) angiotensin-converting enzyme (ACE) activity after 8 weeks of treatment. (d) Serum and (e) heart angiotensin II concentrations after 8 weeks of treatment. Data are means ± standard error of the mean. *$P < 0.05$, **$P < 0.01$.

Effects of Chymase Inhibition on Oxidative Stress in Diabetic Hamsters

We measured the 24-h urinary excretion levels of two oxidative stress markers, 8-OHdG and 8-iso-PGF2α. Urinary 8-OHdG levels were significantly higher in the STZ-induced diabetic hamsters than in the control hamsters ($P < 0.001$), but were significantly reduced by both TEI-F00806 and TEI-E00548 (both, $P < 0.001$ vs STZ; Figure 3a). Similarly, urinary 8-iso-PGF2α levels were significantly higher in STZ-induced diabetic hamsters than in control hamsters ($P < 0.001$), but were significantly reduced by both TEI-F00806 ($P < 0.001$ vs STZ) and TEI-E00548 ($P < 0.01$ vs STZ; Figure 3b). Next, we carried out TBARS assay and immunostaining for 8-OHdG in LV sections of hamsters to evaluate local oxidative stress status in the heart. STZ hamsters showed the significant higher heart MDA levels than control hamsters ($P < 0.05$), and this increase was reduced to the control levels by both TEI-F00806 ($P < 0.05$ vs STZ) and TEI-E00548 ($P < 0.05$ vs STZ; Figure 3c). STZ hamsters showed diffuse, but high, 8-OHdG staining compared with control hamsters, and it was remarkably ameliorated by both chymase inhibitors (Figure 3d–h). We also determined the expression of NOX4, a major source of ROS in the heart, and which is associated with cardiomyopathy in the pressure overload model. In parallel with the accumulation of oxidative stress markers,

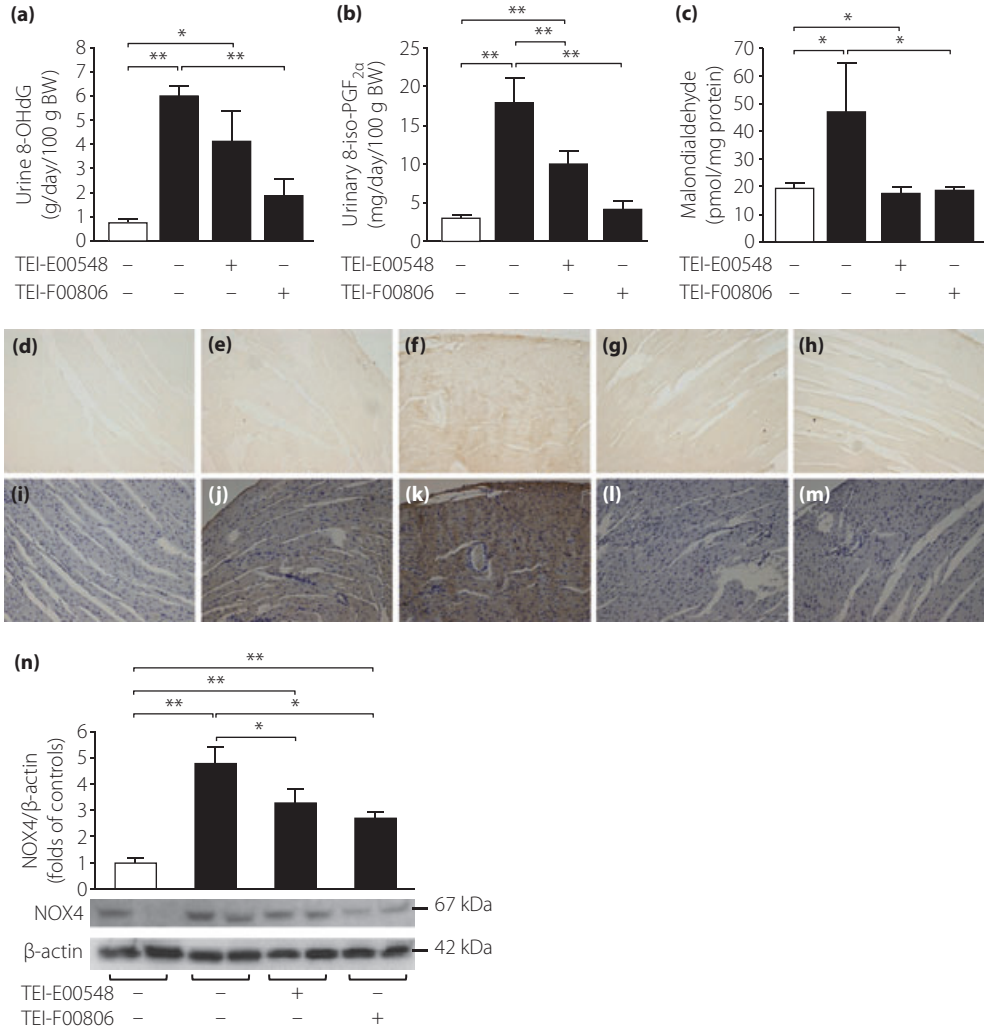

Figure 3 | Effects of chymase inhibition on oxidative stress. White bars: control, non-diabetic controls. Black bars: streptozotocin (STZ), streptozotocin-induced diabetic hamsters. Urinary (a) 8-hydroxy-2′-deoxyguanosine (8-OHdG) and (b) 8-iso-prostaglandin F2α (8-iso-PGF2α) levels adjusted for 24-h urine volume (mL) and bodyweight. (c) Heart malondialdehyde levels adjusted for total protein. Data are means ± SEM. *$P < 0.05$, **$P < 0.01$. (d–h) Immunohistochemistry for 8-OHdG in the heart. Brown, 3,3′-diaminobenzidine tetrahydrochloride stain (8-OHdG). (i–m) Immunohistochemistry for and NOX4 in the heart. Brown, DAB stain (NOX4); blue, hematoxylin counter-staining. (d,i) Negative control, (e,j) control, (f,k) STZ, (g,l) TEI-E00548 or (h,m) TEI-F00806-treated STZ-induced diabetic hamsters (magnification: ×200). (n) Western blotting analysis of NOX4 in the hamster myocardium (quadruplicate samples). The intensity of each NOX4 band was quantified relative to β-actin expression. Results are shown as the fold-change relative to the expression in the control hamsters. Data are means ± standard error of the mean. *$P < 0.05$, **$P < 0.01$ ($n = 8$ per group; ANOVA).

immunostaining analysis for NOX4 showed that the expression of NOX4 was remarkably increased in cardiomyocytes of STZ-induced diabetic hamsters compared with the control hamsters (Figure 3i–m). These increases in NOX4 expression were completely suppressed by both chymase inhibitors (Figure 3l,m). Western blotting analyses of LV tissue homogenates showed that the protein expression of NOX4 was 4.9-fold higher in STZ-induced diabetic hamsters compared with the control hamsters ($P < 0.001$), and this increase was significantly reduced by both TEI-E00548 and TEI-F00806 to the control levels (both, $P < 0.05$ vs STZ; Figure 3n).

Chymase inhibition prevented myocardial fibrosis in diabetic hamsters

We next evaluated the histological changes in the diabetic heart and the effects of chymase inhibition on these changes. Azan staining showed an increase of blue staining representing perivascular and interstitial fibrosis in the myocardium of STZ-induced diabetic hamsters, when compared with the non-diabetic controls. Both TEI-E00548 and TEI-F00806 reduced these histological abnormalities in the diabetic hamsters after 8 weeks of treatment (Figure 4a–d). We then quantified collagen protein accumulation in the tissue sections. As shown in Figure 4b, fibrous accumulation of collagen protein spreading from the vessels to the myocardial tissue was observed in the myocardium of STZ-induced diabetic hamsters, but not in the control hamsters. Both chymase inhibitors decreased the diabetes-induced proliferation of collagen fibers to near control levels (Figure 4e–h). When quantified by absorption photometry, the ratio of collagen to non-collagen staining level in the myocardial sections was significantly higher in the STZ-induced diabetic hamsters than in the control hamsters ($P < 0.01$). Both TEI-E00548 and TEI-F00806 significantly reduced the accumulation of collagen protein in the diabetic heart to control levels (both, $P < 0.05$ vs STZ; Figure 4i). STZ hamsters also showed significantly higher heart hydroxyproline levels than control hamsters ($P < 0.001$), and this increase was reduced to the control levels by both TEI-F00806 ($P < 0.01$ vs STZ) and TEI-E00548 ($P < 0.01$ vs STZ; Figure 4j).

DISCUSSION

In the present study, we showed that myocardial fibrosis in STZ-induced diabetic hamsters was sensitive to chymase inhibition. These histological abnormalities in the diabetic heart occurred in parallel with changes in tissue AngII concentrations, NOX4 expression levels and the accumulation of oxidative stress

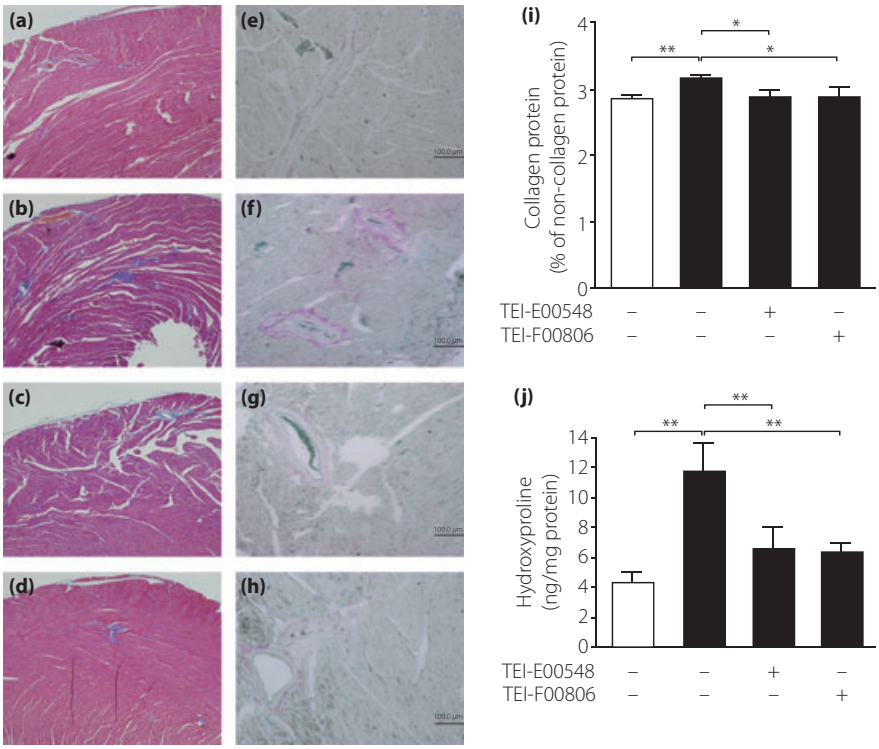

Figure 4 | Effects of chymase inhibition on myocardial fibrosis. (a–d) Azan staining. Red, normal myocardial fiber; blue, myocardial fibrosis and small vessels. (e–h) Collagen staining. Green, non-collagen protein; red, collagen protein. (a,e) Control, (b,f) streptozotocin (STZ), (c,g) TEI-E00548 or (d,h) TEI-F00806-treated STZ-induced diabetic hamsters (magnification: ×200). (i) Ratio of collagen protein to non-collagen protein determined by quantitative analysis with absorption photometry. (j) Heart hydroxyproline levels adjusted for total protein. White bars, control; black bars, STZ. Data are means ± standard error of the mean. *$P < 0.05$, **$P < 0.01$.

markers, and were completely independent of systemic RAS activation.

Human and hamster heart chymases share a common biochemical action in producing AngII from AngI, and are a predominant source of tissue AngII[7,26]. Chymase inhibition suppressed myocardial AngII overproduction, which might be a result of glucose-dependent upregulation of heart chymase in diabetes. However, neither chymase inhibitor affected systemic RAS components. The most likely source of chymase in this model is the mast cells, which store abundant chymase in secretory granules, because immunostaining showed the infiltration and degranulation of chymase-positive inflammatory cells in the pericardial membrane. After its secretion, chymase binds to the extracellular matrix and is active for several weeks[27]. However, the mechanism by which chymase is upregulated in the hyperglycemic state is still unclear. Low-grade inflammation is known to occur in diabetic vascular tissues[28,29], and might induce the infiltration of inflammatory cells, including mast cells. High glucose levels were reported to stimulate ROS production through protein kinase C-dependent activation of NADPH oxidase[16,30]. Furthermore, several reports suggested that fluctuations in glucose levels and the redox state induced mast cell degranulation[31,32]. These findings suggest that tissue chymase might be released by proliferating mast cells in uncontrolled diabetes.

In the heart, inflammatory cells are also involved in the proliferation of fibroblasts and the generation of collagen as sources of not only inflammatory cytokines, but also serine proteases, such as cathepsin G, ACE and chymase, cleaving AngI to AngII in heart tissue. In particular, chymase was reported to predominate over ACE activity in the human heart, accounting for extremely high total AngII formation in humans compared with other species[33]. Thus, the upregulation of heart chymase might play the primary role in the AngII overgeneration, leading to fibrous changes in the diabetic heart.

It is well established that AngII stimulates ROS production by activating or increasing the expression of NADPH oxidase in vascular cells. Previously, we showed that the expression of NOX4, a major component of NADPH oxidase, was clearly correlated to renal AngII level in kidneys of diabetic hamsters, and that chymase-specific inhibitors attenuated oxidative stress and normalized the expression of NOX4 in diabetic nephropathy[23]. The results of the present study support those of recent studies showing that NOX4-induced oxidative stress predominantly contributed to the development of LV dysfunction[11,12], and that the pathogenic effects of NADPH oxidase-derived oxidative stress were applicable to diabetic cardiomyopathy, as well as other complications. In contrast, Zhang *et al.*[34] have shown that NOX4 protects against chronic load-induced hypoxic stress in mouse hearts. The pathophysiological role of NOX4 in ROS imbalances under the other stress conditions still remains controversial.

The limitations of the present study are that we did not assess LV function and we used a model of type 1 diabetes. As a substitute for cardiac function analysis, we evaluated the histological changes of the myocardium. Previous reports showed that myocardial fibrosis was related to LV function in STZ-induced diabetic models with a similar duration of hyperglycemia[5,14]. The latter limitation is a result of the lack of type 2 diabetic hamster models. However, a hamster model was essential for the present study, because chymases in other rodents are known to degrade AngII, unlike human chymases[7,26].

In conclusion, chymase inhibition was sufficient to prevent myocardial fibrosis in diabetes and might be a promising intervention to prevent diabetic cardiomyopathy during the early stage of onset. The effectiveness of chymase-specific inhibitors should be further confirmed in human trials.

ACKNOWLEDGEMENTS

The authors thank Teijin Pharma Ltd for supplying TEI-E00548 and TEI-F00806. We also thank the staff at the Research Support Center, Graduate School of Medical Sciences, Kyushu University, for technical support. This work was supported by a Grant-in-Aid for Scientific Research (No.16590888) from the Ministry of Education, Culture, Sports, Science and Technology (MEXT), Japan, and by Special Coordination Funds for Promoting Science and Technology (SCF; Funding program 'Innovation Center for Medical Redox Navigation'). No conflicts of interest are declared by the authors.

REFERENCES

1. MacDonald MR, Petrie MC, Varyani F, *et al.* Impact of diabetes on outcomes in patients with low and preserved ejection fraction heart failure: an analysis of the Candesartan in Heart failure: Assessment of Reduction in Mortality and morbidity (CHARM) programme. *Eur Heart J* 2008; 29: 1377–1385.
2. Pfeffer MA, Swedberg K, Granger CB, *et al.* Effects of candesartan on mortality and morbidity in patients with chronic heart failure: the CHARM-Overall programme. *Lancet* 2003; 362: 759–766.
3. Cice G, Di Benedetto A, D'Isa S, *et al.* Effects of telmisartan added to angiotensin-converting enzyme inhibitors on mortality and morbidity in hemodialysis patients with chronic heart failure: a double-blind, placebo-controlled trial. *J Am Coll Cardiol* 2010; 56: 1701.
4. Brenner BM, Cooper ME, de Zeeuw D, *et al.* Effects of losartan on renal and cardiovascular outcomes in patients with type 2 diabetes and nephropathy. *N Engl J Med* 2001; 345: 861–869.
5. Fiordaliso F, Li B, Latini R, *et al.* Myocyte death in streptozotocin-induced diabetes in rats in angiotensin II-dependent. *Lab Invest* 2000; 80: 513–527.
6. Frustaci A, Kajstura J, Chimenti C, *et al.* Myocardial cell death in human diabetes. *Circ Res* 2000; 87: 1123–1132.
7. Kinoshita A, Urata H, Bumpus FM, *et al.* Multiple determinants for the high substrate specificity of an angiotensin II-forming chymase from the human heart. *J Biol Chem* 1991; 266: 19192–19197.

8. Ihara M, Urata H, Shirai K, *et al.* High cardiac angiotensin-II-forming activity in infarcted and non-infarcted human myocardium. *Cardiology* 2000; 94: 247–253.
9. Shiota N, Jin D, Takai S, *et al.* Chymase is activated in the hamster heart following ventricular fibrosis during the chronic stage of hypertension. *FEBS Lett* 1997; 406: 301–304.
10. Hoshino F, Urata H, Inoue Y, *et al.* Chymase inhibitor improves survival in hamsters with myocardial infarction. *J Cardiovasc Pharmacol* 2003; 41(Suppl. 1): S11–S18.
11. Ago T, Kuroda J, Pain J, *et al.* Upregulation of Nox4 by hypertrophic stimuli promotes apoptosis and mitochondrial dysfunction in cardiac myocytes. *Circ Res* 2010; 106: 1253–1264.
12. Kuroda J, Ago T, Matsushima S, *et al.* NADPH oxidase 4 (Nox4) is a major source of oxidative stress in the failing heart. *Proc Natl Acad Sci USA* 2010; 107: 15565.
13. Baynes JW. Role of oxidative stress in development of complications in diabetes. *Diabetes* 1991; 40: 405–412.
14. Kajstura J, Fiordaliso F, Andreoli AM, *et al.* IGF-1 overexpression inhibits the development of diabetic cardiomyopathy and angiotensin II-mediated oxidative stress. *Diabetes* 2001; 50: 1414–1424.
15. Crespo MJ, Zalacain J, Dunbar DC, *et al.* Cardiac oxidative stress is elevated at the onset of dilated cardiomyopathy in streptozotocin-diabetic rats. *J Cardiovasc Pharmacol Ther* 2008; 13: 64–71.
16. Inoguchi T. High glucose level and free fatty acid stimulate reactive oxygen species production through protein kinase C–dependent activation of NAD (P) H oxidase in cultured vascular cells. *Diabetes* 2000; 49: 1939–1945.
17. Geiszt M, Kopp JB, Varnai P, *et al.* Identification of renox, an NADPH oxidase in kidney. *Proc Natl Acad Sci USA* 2000; 97: 8010–8014.
18. Shiose A, Kuroda J, Tsuruya K, *et al.* A novel superoxide-producing NADPH oxidase in kidney. *J Biol Chem* 2001; 276: 1417–1423.
19. Cai L, Wang Y, Zhou G, *et al.* Attenuation by metallothionein of early cardiac cell death via suppression of mitochondrial oxidative stress results in a prevention of diabetic cardiomyopathy. *J Am Coll Cardiol* 2006; 48: 1688–1697.
20. Li CJ, Zhang QM, Li MZ, *et al.* Attenuation of myocardial apoptosis by alpha-lipoic acid through suppression of mitochondrial oxidative stress to reduce diabetic cardiomyopathy. *Chin Med J (Engl)* 2009; 122: 2580–2586.
21. Mollnau H, Wendt M, Szocs K, *et al.* Effects of angiotensin II infusion on the expression and function of NADPH oxidase and components of nitric oxide/cGMP signaling. *Circ Res* 2002; 90: E58–E65.
22. Etoh T, Inoguchi T, Kakimoto M, *et al.* Increased expression of NADPH oxidase subunits, NOX4 and p22phox, in the kidney of streptozotocin-induced diabetic rats and its reversibity by interventive insulin treatment. *Diabetologia* 2003; 46: 1428–1437.
23. Maeda Y, Inoguchi T, Takei R, *et al.* Inhibition of chymase protects against diabetes-induced oxidative stress and renal dysfunction in hamsters. *Am J Physiol Renal Physiol* 2010; 299: F1328–F1338.
24. Jimenez W, Pares A, Caballeria J, *et al.* Measurement of fibrosis in needle liver biopsies: evaluation of a colorimetric method. *Hepatology* 1985; 5: 815–818.
25. Kobori H, Nishiyama A, Harrison-Bernard LM, *et al.* Urinary angiotensinogen as an indicator of intrarenal Angiotensin status in hypertension. *Hypertension* 2003; 41: 42–49.
26. Akasu M, Urata H, Kinoshita A, *et al.* Differences in tissue angiotensin II-forming pathways by species and organs in vitro. *Hypertension* 1998; 32: 514–520.
27. Miyazaki M, Takai S, Jin D, *et al.* Pathological roles of angiotensin II produced by mast cell chymase and the effects of chymase inhibition in animal models. *Pharmacol Ther* 2006; 112: 668–676.
28. Danesh J, Wheeler JG, Hirschfield GM, *et al.* C-reactive protein and other circulating markers of inflammation in the prediction of coronary heart disease. *N Engl J Med* 2004; 350: 1387–1397.
29. Zhang LF, Zalewski A, Liu Y, *et al.* Diabetes-induced oxidative stress and low-grade inflammation in porcine coronary arteries. *Circulation* 2003; 108: 472.
30. Inoguchi T, Sonta T, Tsubouchi H, *et al.* Protein kinase c-dependent increase in reactive oxygen species (ROS) production in vascular tissues of diabetes: role of vascular NAD (P) H oxidase. *J Am Soc Nephrol* 2003; 14(8 Suppl 3): S227–S232.
31. Wolfreys K, Oliveira DBG. Alterations in intracellular reactive oxygen species generation and redox potential modulate mast cell function. *Eur J Immunol* 1997; 27: 297–306.
32. Hu W, Shen Y, Fu Q, *et al.* Effect of oxygen-glucose deprivation on degranulation and histamine release of mast cells. *Cell Tissue Res* 2005; 322: 437–441.
33. Balcells E, Meng QC, Johnson WH, *et al.* Angiotensin II formation from ACE and chymase in human and animal hearts: methods and species considerations. *Am J Physiol* 1997; 2: H1769–H1774.
34. Zhang M, Brewer AC, Schroder K, *et al.* NADPH oxidase-4 mediates protection against chronic load-induced stress in mouse hearts by enhancing angiogenesis. *Proc Natl Acad Sci USA* 2010; 107: 18121–18126.